Recombination Investigation of InGaP HBT's

B.-K. Han, A. Wibowo, V. Tu, G. Du, and N. Pan

MicroLink Devices, 6457 Howard Street, Niles, IL 60201, USA
E-mail: bhan@mldevices.com Phone: (847) 588-3001

Keywords: InGaP, Heterojunction Bipolar Transistor, Recombination, Burn-in, Reliability

Abstract

We demonstrated InGaP/GaAs heterojunction bipolar transistors (HBT's) with very low burn-in and high β/R_{sB} ratios by optimization of emitter and base properties and *in situ* annealing. Some HBT's exhibited β/R_{sB} ratios of 0.47 and less than 5% burn-in. The recombination analysis of the devices revealed that the emitter and emitter-base junction were unaffected from the burn-in reduction annealing. The devices were then stressed at T_j = 210ºC and current density, 12.5 kA/cm^2 for 48 hours. The devices that were carefully optimized showed very little degradation on gain and base-emitter junctions. Some devices showed more pronounced degradation on emitter-base junction, that were similar to Gummel curves of an early stage of failed devices during the DC accelerated lifetime test.

INTRODUCTION

InGaP/GaAs heterojunction bipolar transistors (HBT's) have been widely used in high frequency and high power wireless applications. The requirement of higher bandwidth data rates such as EDGE has resulted in the need of higher performance power amplifiers. [1] These applications often require higher performance, stability and reliability of HBT's. HBT's by means of metalorganic chemical vapor deposition (MOCVD) traditionally exhibit two types of DC transient characteristics; Burn-in (BI) and gain degradation during accelerated lifetime tests.[2-9] These changes in DC characteristics can change RF output characteristics and performance. This raises efforts to reduce BI and gain degradation in order to control quality of device performance and stability during the lifetime operation of the devices.

In the past, there have been numerous works to reduce the BI characteristics.[5-8] The process usually employed annealing steps *in situ* during the epitaxial process or *ex situ* during the device fabrication. Typically, these annealed devices usually resulted in severe gain degradation and/or poor reliability. There have been many studies trying to investigate the causes of the BI phenomenon and degraded gain. Much effort has been focused on analyzing recombination on bulk and surfaces of base and emitter.[10-12] There have been several theories on where the sources of the burn-in and gain degradation are. So far, the consensus has yet to be achieved.

Models such as

$$\frac{1}{\beta}=\frac{I_B}{I_C}=\frac{J_{bulk}}{J_c}+\frac{J_{scr}}{J_c}+\frac{Jsr}{Jc}\bullet\frac{P}{A}=\frac{1}{\beta_0}+\frac{Jsr}{Jc}\bullet\frac{P}{A}$$

have been used to investigate correlations between surface recombination (sr) currents and the emitter geometry.[5,10-12] This model provides a good insight on how much surface recombination contribute to base current at low bias. However, it is difficult to assess contribution for the space-charge-recombination (scr) from this model since it lumps scr and neutral-base-recombination (nbr) components. The equation needs a modification in order to differentiate scr and nbr components. Hattori et. al. recently demonstrated a model of $1/\beta$ and $1/(Jc^{1/2})$ that can easily separate all components.[13]

This model employs

$$I_C = S_E J_{co}\exp(qV_{BE}/n_3kT)$$
$$I_B = S_E J_{nbr}\exp(qV_{BE}/n_1kT)+ (S_E J_{scr}+L_E J_{sr})\exp(qV_{BE}/n_2kT)$$
$$I_B/I_C = 1/\beta = 1/\beta_o + \frac{S_E J_{scr}+L_E J_{sr}}{S_E (J_{co})^{(n_3/n_2)}} J_c^{(n_3/n_2-1)}$$

where S_E and L_E are emitter area and perimeter, respectively. The equation can be further reduced by assuming that $n_1 \approx 1$, $n_2 \approx 2$, and $n_3 \approx 1$. A simplified equation can be obtained as

$$1/\beta = 1/\beta_o + grad\bullet J_c^{-0.5} \quad (1)$$

where

$$grad=\frac{S_E J_{scr}+L_E J_{sr}}{S_E\sqrt{J_{co}}}.$$

Applying this model to HBT's of emitters with various geometries, one can isolate individual components for neutral base, space-charge and surface recombination currents. Using this information, one may identify possible causes that contribute to the degradation of device performance and stability, such as burin-in and gain degradation during the normal and accelerated stress operation.

In this paper, we present investigation of the BI phenomenon in relations to base and emitter impurity concentrations, and *in situ* annealing. We also present devices that were optimized for the reduced burn-in and gain shift under high temperature and high current density operation, using the recombination model described above.

DEVICE STRUCTURES AND FABRICATION

InGaP/GaAs HBT's were grown on a GaAs semi-insulating 2 deg off (100) substrates with an AIXTRON 2600G3 multi-wafer MOCVD reactor. The general structures consisted of a 500 A un-doped GaAs layer, a 6000 Å n-GaAs subcollector layer with silicon doping at Nd = $4x10^{18}$ cm^{-3}, a thick Å n-GaAs collector layer, a p+-GaAs base layers with carbon doping, a 400 Å n-InGaP emitter layer with silicon doping, a 1000 Å n+-GaAs emitter cap layer with silicon doping at Nd = $4x10^{18}$ cm^{-3}, a 500 Å graded n-InGaAs layer with tellurium doping at $1x10^{19}$ cm^{-3} and a 500 Å n+-InGaAs contact layer with tellurium doping at $2x10^{19}$ cm^{-3}. In situ annealing was performed during the deposition process at various temperature and periods in order to reduce BI transients. The description of emitter and base layers 6 devices are shown in Table 1. Lower burn-in generally corresponds to longer or higher *in situ* annealing temperature.

TABLE I
BURN-IN, BASE AND EMITTER DOPING CONCENTRATIONS OF HBT'S

Device	Base doping ($x10^{19}$ cm^{-3})	Emitter doping ($x10^{17}$ cm^{-3})	Burn-in %	β/R_{sB} Ratio
A	4	5	37	0.54
B	4	3	3	0.45
C	3	3	49	0.58
D	3	3	12	0.55
E	3	3	5	0.47
F	3	3	3	0.42

Two types of discrete devices were fabricated. Unpassivated discrete large area devices with emitter size of 75 x 75 μm^2 were initially fabricated to ensure the devices structures and parameters. Small area devices with emitter size of 4 x 20 μm^2 were fabricated using non-self aligned process. Emitter ledges and external base was passivated with CVD nitride. Ti/Pt/Au metal was deposited to form the base and emitter contacts. AuGe/Ni/Au was used for the collector contacts. The devices were tested on wafer at room temperature for standard DC measurements. Gummel curves of all devices stabilized after five IV sweeps. BI was measured after comparing the first Gummel plots and the fifth Gummel plots.

The devices were then stressed under T_j = 210ºC and emitter current density, 12.5 kA/cm^2 for 48 hours. The stress was relieved at times and measurements were carried out at room temperature. The DC current gain changes and transients of base currents of the devices are monitored and compared.

RESULTS AND DISCUSSION

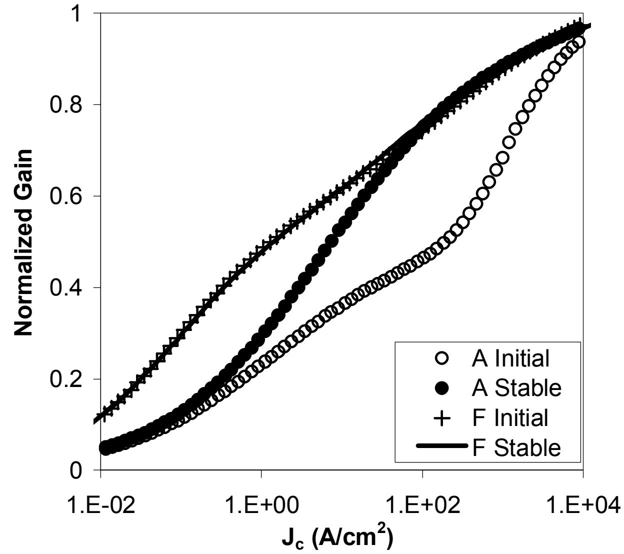

Figure 1. Normalized DC current gain transients of sample A and sample F. Samples A and F show 37% BI and 3% BI, respectively. (L=4x20 μm^2)

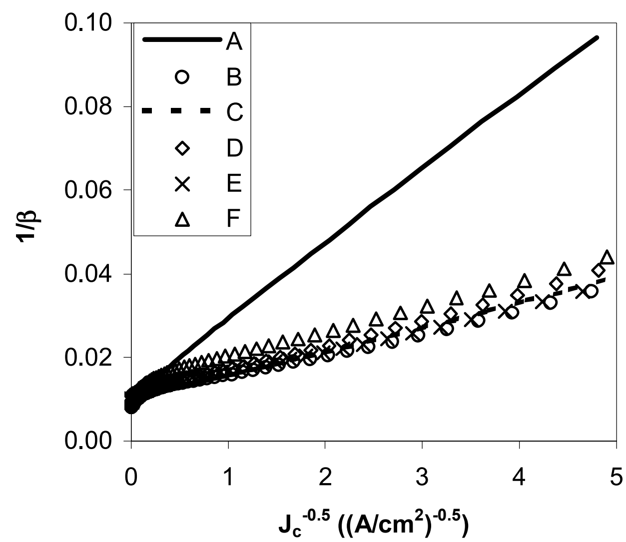

Figure 2. Base and EB junction components extracted from the stabilized Gummel traces of the six samples. The slopes are proportional to J_{scr} and J_{sr}. Intercept correlates to J_{nbr}.. (L=4x20 μm^2)

The gain transients of sample A and sample F are shown in Figure 1, as an example. The burn-in amount varies with current density. The devices tested in this experiment usually reach maximum BI near 200 A/cm^2. Thus, we reported BI percentages in Table 1 measured at 200 A/cm2 at room temperature and calculated from $(\beta_5-\beta_1)/\beta_5$.

Gummel curves for all devices show very little shift on I_c for room temperature IV measurements. All devices resulted in DC current gain of approximately 100 measured at 1 kA/cm^2. The β/R_{sb} ratios for devices A, B, C, D, E, and F were 0.54, 0.45, 0.58, 0.55, 0.47 and 0.42, respectively. DC gains in sample D and E are some of the highest β/R_{sB} ratios reported for devices with the burn-in reduction annealing. This is a significant improvement from previously reported results since BI suppression annealing usually resulted in drastic reduction of β/R_{sb} ratios.[5-8]

Gain (β) and J_c of stabilized devices are re-plotted to $1/\beta$ and $J_c^{-0.5}$ curves shown on Figure 2. The slope of each curve is proportional to J_{scr} and J_{sr}. The Y-intercept correlates to J_{nbr}. The slope of sample A, which composed of higher emitter doping concentration, is significantly higher than slopes for other samples whereas Y-intercepts are very similar to all devices. The results indicate that J_{scr} and J_{sr} components of sample A are higher than those of samples B thru F, whereas J_{nbr}'s of all devices are very similar.

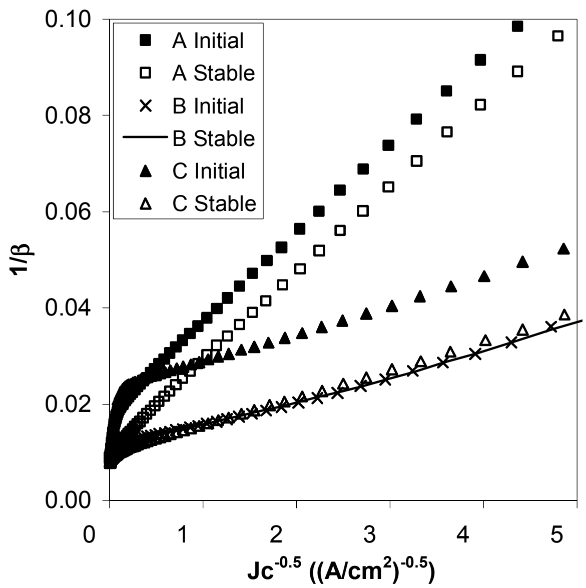

Figure 3. Base and EB junction components extracted from the initial and stabilized Gummel curves from devices A, B, and C. Slopes do not change during the burn-in stabilization. Linearly extrapolated Y-Intercepts from initial IV sweep of samples A (37% BI) and C (49% BI) are higher than Y-intercepts from stabilized devices. Sample B (3 % BI) shows very little shifts after the burn-in. (L=4x20 μm^2)

Shown in Figure 3, are the $1/\beta$ and $J_c^{-0.5}$ graph extracted from Gummel curves of the initial and the stabilized test devices. Linearly extrapolated Y-intercepts of sample A and C shift down after the burn-in, and Y-intercepts of sample B is barely moved. Although not shown, changes of Y-intercepts of samples D, E and F all corresponded very closely to the BI percentages. Since the slopes of the curves are unchanged, it is evident that J_{scr} and J_{sr} components are not influenced during the burn-in stabilization.

Combining the results from Figure 2 and Figure 3, we determined that the J_{scr} and J_{sr} of all devices in this experiment were independent from current gain, degree of burn-in, and burn-in reduction annealing. *In situ* annealing reduced the burn-in and β/R_{sB} ratios of the devices, which translates to shorter minority carrier lifetime in the base caused by degradation of the base material. This trend correlates with other reports.[6,8,9] However, the fact that β/R_{sB} ratios are high and burn-in percentages are low, and that J_{scr} and J_{sr} are un-compromised indicate that our burn-in reduction annealing is well optimized.

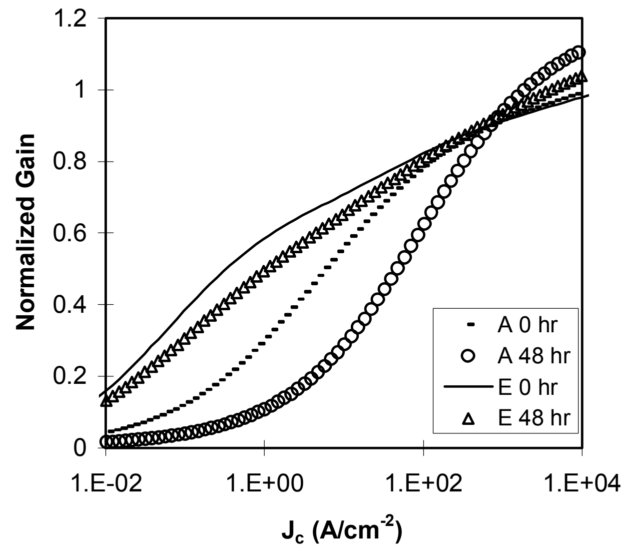

Figure 4. Normalized DC current gain of samples A and E after stressing at T_j = 210ºC and current density, 12.5 kA/cm² for 48 hours. DC current gain shift at 200 A/cm² for Samples A and E are -13% and -1%, respectively. DC current gain shift at 12.5 kA/cm² for Samples A and E are 12% and 6%, respectively. (L = 4 x 20 μm^2)

TABLE 2

CHANGE OF DC CURRENT GAIN AFTER 48-HOUR STRESS

	200 A/cm²	1 kA/cm²	12.5 kA/cm²
A	0.87	1.02	1.12
B	0.57	0.79	1.08
C	1.19	1.19	1.19
D	1.05	1.07	1.09
E	0.99	1.02	1.06
F	0.89	0.93	1.00

After the devices were stabilized, they were stressed at T_j = 210ºC and current density, 12.5 kA/cm² for 48 hours. Figure 4 displays normalized gains of samples A and E as example. We noticed that the DC current gain changed as the devices were stressed. The DC current gains drifted up or down depending on the current densities, burn-in percentages, and the doping concentrations of the base and emitter. The changes of the DC current gain on three current densities are reported in Table 2. Generally, DC current gain of devices with low burn-in increased little (<10%) at high current density (>1kA/cm²). Devices with high base doping (A and B) showed drastic decrease in the DC current gain at lower current density (<1kA/cm²). Devices with low base doping concentration showed little or mild changes at lower currently density (<1kA/cm²).

Upon recombination analysis of the stressed devices, it was revealed that devices with high base ($4x10^{19}$ cm^{-3}) and high emitter doping concentration ($5x10^{17}$ cm^{-3}) showed rapid rise of J_{scr} and J_{sr} components. J_{nbr} also increased for the devices whose gains at >1kA/cm^2 increased during the stress test. The burn-in reduction annealing influenced the J_{scr} and J_{sr}, but the rate of rise was very small compared to effects by high base and emitter doping concentrations. The Gummel curves of sample A resemble early stage Gummel curves of samples that failed during the accelerated lifetime test.[3,4,9] It is possible that devices with rapid rises of J_{scr} and J_{sr} components during the stress test can result in poor reliability due to early degradation of emitters, since emitter degradation is one of major failure mechanisms of HBT's reliability.[4,9] However, further work has to be done to determine if those devices would fail the accelerated DC lifetime test. It is then feasible that HBT's with longer lifetime and better stability can be obtained by careful optimization of doping concentrations of emitter and base, and burn-in reduction annealing.

SUMMARY

In summary, we have demonstrated HBT's with very low burn-in and high β/R_{sB} ratios. This was achieved by careful optimization of in situ annealing, device structures, and recombination analysis. Optimized devices also showed mild gain transients during the stress test that simulated DC accelerated reliability test.

ACKNOWLEDGEMENTS

The authors would like to thank the Mr. R. Hattori, Mr. Y. Yamamoto, Mr. S. Suzuki, Mr. T. Shimura, and Mr. Ogawa from Mitsubishi Electric Corporation for helpful discussions and for application of recombination analysis models. We would also like to thank Dr. Thomas Low of Agilent Technologies for his technical support and discussions to improve HBT devices. We are grateful for the unconditional support from Dr. Y. Kodo to develop advanced HBT.

REFERENCES

[1] K. Yamamoto, et al., *A GSM/EDGE Dual-Mode, 900/1800/1900-MHz Triple-Band HBT MMIC Power Amplifier Module,* 2002 IEEE Radio Frequency Integrated Circuits Symposium Digest, pp. 245-248, 2002.

[2] A.A. Rezazadeh, et al., *Bias and Temperature Stress Reliability of InGaP/GaAs HBTs,* IEEE 38th Annual International Reliability Physics Symposium Digest, pp. 250-257, 2000.

[3] E.F. Yu, et al., *Reliability Implication of InGaP HBT Emitter Ledge Dimension,* JEDEC, pp. 167-174, 2002.

[4] N. Pan, et al., *Reliability of InGaP and AlGaAs HBT,* IEICE Trans. on Electronics, vol. E84-C, No. 10, pp. 1366-1372, October 2001.

[5] K-K. Chong, et al., *Suppression of the burn-in effect in InGaP/GaAs heterojunction bipolar transistors by constant period of voltage stress,* Journal of Applied Physics, vol. 95, No. 4, pp. 2079-2083, February 2004.

[6] J. Mimila-Arroyo, et al., *Dependence of burn-in effect on thermal annealing of the GaAs:C base layer in GaInP heterojunction bipolar transistors,* Applied. Physics Letters, vol. 82, No. 17, pp. 2910-2912, April 2003.

[7] J. Mimila-Arroyo, *Burn-in effect on GaInP heterojunction bipolar transistors,* Applied. Physics Letters, vol. 83, No. 15, pp. 3204-3206, October 2003.

[8] Q. Yang, et al., *Minority carrier lifetime degradation in carbon-doped base of InGaP/GaAs heterojunction bipolar transistors grown by low-pressure metalorganic chemical vapor deposition,* Applied. Physics Letters, vol. 77, No. 2, pp. 271-273, July 2000.

[9] R. E. Welser, et al., *Exploring Physical Mechanisms for Sudden Beta Degradation in GaAs-based HBTs,* JEDEC, pp. 135-138, 2001.

[10] N. Hayama, et al., *Emitter Size Effect on Current Gain in Fully Self-Aligned AlGaAs/GaAs HBTs with AlGaAs Surface Passivation Layer,* IEEE Electron Device Letters, vol. 11, No. 9, pp. 388-390, September 1990.

[11] Y. F. Yang, et al., *Surface Recombination Current in InGaP/GaAs Hetrostructure-Emitter Bipolar Transistors,* IEEE Trans. on Electron Devices, vol. 41, No. 5, pp. 643-647, May 1994.

[12] T. Henderson, et al., *Base-emitter leakage and recombination current in an implant isolated region of a GaAs/AlGaAs heterojunction bipolar transistor,* Journal of Applied Physics, vol. 72, No. 11, pp. 5489-5492, December 1992.

[13] R. Hattori, et al., *Manufacturing Technology of InGaP HBT Power Amplifiers for Cellular Phone Applications,* 2002 GaAs MANTECH Digest of Papers, pp. 241-242, April 2002.